homeless is required for RNA localization in *Drosophila* oogenesis and encodes a new member of the DE-H family of RNA-dependent ATPases

Doreen E. Gillespie and Celeste A. Berg[1]

University of Washington, Department of Genetics, Seattle, Washington 98195-7360

The *homeless* (*hls*) gene of *Drosophila* is required for anteroposterior and dorsoventral axis formation during oogenesis. At a low frequency, females homozygous for mutations in *hls* generate early egg chambers in which the oocyte is positioned incorrectly within the cyst. At a high frequency, late-stage egg chambers exhibit a ventralized chorion. Sequence analysis of the *hls* cDNA predicts a protein with amino-terminal homology to members of the DE-H family of RNA-dependent ATPases and putative helicases. Similarity of 51% in the amino-terminal third of the protein was found to two yeast splicing factors, PRP2 and PRP16, and to *Drosophila* Maleless, which is required for dosage compensation. To analyze Hls function, RNA localization patterns were determined for seven different transcripts in *hls* mutant ovaries. Previtellogenic transport to the oocyte was unaffected for all transcripts examined. Transport and localization of *bicoid* and *oskar* messages during vitellogenic stages were strongly disrupted, and the distribution and/or quantity of *gurken*, *orb*, and *fs(1)K10* mRNAs were also affected, but to a lesser degree. In contrast, *hu-li tai shao* and *Bicaudal-D* transcripts were transported and localized normally in *hls* mutants. In addition, Kinesin heavy chain:β-Galactosidase fusion protein failed to localize correctly to the posterior of the oocyte in vitellogenic egg chambers. Examination of the microtubule structure with anti-α-Tubulin antibodies revealed aberrant microtubule organizing center movement and an abnormally dense cytoplasmic microtubule meshwork. We discuss potential roles for Hls in organizing a cytoskeletal framework essential for localizing specific RNAs.

[*Key Words*: Localized RNA; RNA-binding protein; anterior/posterior axis; dorsal/ventral axis; microtubule; germ line]

Received April 25, 1995; revised version accepted August 29, 1995.

The rapid development of the *Drosophila* embryo is facilitated by the establishment of the anteroposterior (a/p) and dorsoventral (d/v) axes during oogenesis. The *Drosophila* egg is formed from an egg chamber composed of 16 interconnected germ-line cells surrounded by somatic follicle cells (for review, see Spradling 1993). By stage 1 (S1) of oogenesis, the oocyte has been determined and has moved from a central location to the posterior of the 16-cell cyst. The *egalitarian*, *Bicaudal-D* (*Bic-D*), and *hu-li tai shao* (*hts*) genes are required to specify the oocyte within the cyst (Steward and Nüsslein-Volhard 1986; Schüpbach and Wieschaus 1991; Yue and Spradling 1992; Ran et al. 1994), whereas *dicephalic* (*dic*), *spindle-C*, and *armadillo* function in positioning the oocyte at the posterior of the egg chamber (Lohs-Schardin 1982; Peifer et al. 1993; González-Reyes and St. Johnston 1994). Cytoskeletal architecture within the egg chamber is important for oocyte determination and positioning, as well as for the localization of mRNAs and proteins involved in a/p and d/v axis formation (Koch and Spitzer 1983; Pokrywka and Stephenson 1991, 1995; Theurkauf et al. 1993; Lin et al. 1994; González-Reyes et al. 1995; Roth et al. 1995; for review, see Theurkauf 1994a).

The 15 nurse cells at the anterior of the developing egg chamber produce RNAs and proteins necessary for the formation and maintenance of the a/p and d/v axes within the oocyte, as well as proteins and organelles that provide essential cellular and developmental functions during embryogenesis. Subcellular localization of the axis-determining RNAs and proteins is important for proper development. This localization requires efficient transport through the nurse cells and oocyte and subsequent anchoring or stabilization within the oocyte. For example, transcripts for the anterior embryonic determinant Bicoid (Bcd) require Exuperantia (Exu), Swallow (Swa), and Staufen (Stau) proteins for transport to, and localization within, the oocyte (for review, see St. Johnston et al. 1989; Stephenson and Pokrywka 1992).

[1]Corresponding author.

Transcripts of the posterior determinant Nanos are localized through the activities of the posterior group genes whose products make up the polar granules found at the posterior of the embryo (Mahowald 1962; Wang and Lehmann 1991; for review, see St. Johnston 1993). The first step is the colocalization of Stau protein and *oskar* (*osk*) mRNA to the posterior of the oocyte at S8. Localization of each additional component occurs in a stepwise fashion and requires the activity of the earlier genes (Lehmann and Nüsslein-Volhard 1991; for review, see St. Johnston 1993). Both processes, localization of *bcd* mRNA to the anterior of the oocyte and localization of *osk* mRNA and Stau protein to the posterior of the oocyte, depend on an organized microtubule network whose orientation is defined by a reciprocal cell-signaling process between germ cells and follicle cells (Pokrywka and Stephenson 1991; Clark et al. 1994; González-Reyes et al. 1995; Roth et al. 1995). This signaling cascade requires the activity of Gurken (Grk), a transforming growth factor-α (TGF-α)-like molecule, and Cornichon (Cni), whose precise molecular function is not known, to act in the germ line and signal to the polar follicle cells (González-Reyes et al. 1995; Roth et al. 1995). Reception of the signal via the epidermal growth factor (EGF)-receptor homolog Torpedo (Top) establishes their fate as posterior. Subsequent signaling from the posterior follicle cells back to the oocyte in a Protein kinase A (PKA)-mediated fashion directs the organization of the microtubule network and leads to the proper localization of embryonic determinants (Ruohola et al. 1991; Lane and Kalderon 1994).

The establishment of the dorsoventral axis also involves localized RNAs and proteins. The first visual manifestation of dorsoventral polarity within the oocyte is the movement of the oocyte nucleus toward the dorsal side of the egg chamber, also via a microtubule-dependent mechanism (Koch and Spitzer 1983; González-Reyes et al. 1995; Roth et al. 1995). Subsequently, *grk* transcripts are localized tightly to the anterodorsal cortex of the oocyte, overlying the oocyte nucleus, in a process dependent on the function of the *cappucino*, *spire*, *fs(1)K10* (*K10*), *squid*, and *orb* genes (Neuman-Silberberg and Schüpbach 1993; Christerson and McKearin 1994). Reception of the Grk signal via the EGF receptor in the dorsal follicle cells is required for the synthesis of dorsal eggshell structures and the establishment of dorsoventral polarity in the embryo (Chasan and Anderson 1993; for review, see Schüpbach and Roth 1994). Thus, the *grk* pathway acts in establishing both a/p and d/v polarity (for review, see Anderson 1995).

Characterization of RNA localization mechanisms that function in other developmental processes has revealed a selective dependence on cytoskeletal structures. Two basic mechanisms have been described: active transport and anchoring of a message or uniform distribution followed by specific degradation. In a developing *Drosophila* egg chamber, for example, a/p polarity is inherently provided by the relationship of the nurse cells to the oocyte. An transcript entering the oocyte from the nurse cells must enter at the anterior end and, thus, has an efficient staging platform for either retention in the anterior region or specific transport to the posterior pole. In this way, *osk* and *bcd* mRNAs are distinguished and differentially localized. Some transcripts, however, are localized in an indirect manner, for example, *Hsp83* RNA. Transcripts of *Hsp83* are transported from the nurse cells to the oocyte and are diffuse throughout the oocyte until fertilization. At that time, posterior *Hsp83* message is protected and the remainder is degraded (Ding et al. 1993a). No role for microtubule scaffolding in *Hsp83* message localization has been demonstrated. Similarly, in a *Xenopus* oocyte, which develops without nurse cells, microtubule organization is critical for the localization of some mRNAs but not others. Diffuse messages of *Vg1* are localized to the vegetal pole through a microtubule-dependent process (Yisraeli et al. 1990). Subsequent anchoring requires intermediate filaments—cytoskeletal components not found in *Drosophila*. In contrast, transport of *Xlsirts*, *Xcat2*, and *Xwnt11* mRNAs, also localized to the vegetal pole during oogenesis, is resistant to both nocodazole and cytochalasin B, suggesting that neither actin nor microtubules are components of the transport mechanisms for these transcripts (Kloc and Etkin 1995). Microtubules also have been implicated in RNA localization in fully differentiated mammalian neuronal cells. *tau* message, for example, is localized to the cell body and proximal axon region and is associated with the microtubule fraction of extracted cells; tubulin transcripts, restricted to the cell body, do not associate with microtubules (Litman et al. 1994).

The machinery required for RNA localization must provide specificity in transport, localization, and stabilization or degradation, as necessary. In this paper we describe the *homeless* (*hls*) gene, whose product is necessary for correct RNA localization during *Drosophila* oogenesis.

Results

Isolation of hls *mutants*

In a large scale P{*lacZ,ry*$^+$} screen (described in Karpen and Spradling 1992), we obtained a female sterile line, *3987*, in which the P element mapped by in situ hybridization to 89A5,6. Females homozygous for the insertion laid few eggs, and these appeared to be unfertilized. Upon dissection of the ovaries from these females, we observed defects at two stages of oogenesis. At a low frequency, vitellogenic egg chambers were produced in which the oocyte was not located at the usual posterior position in the egg (Fig. 1). In addition, 95% of late-stage egg chambers were ventralized, at least partially (Fig. 2). We also observed a small number of degenerating egg chambers at all stages (Table 1). We have named the gene *hls* based partly on the oocyte mislocalization phenotype and partly on the RNA localization phenotype described in subsequent sections of this paper. Females transheterozygous for *hls*^{3987} and any of a number of deficiencies uncovering the region (see Materials and methods) pro-

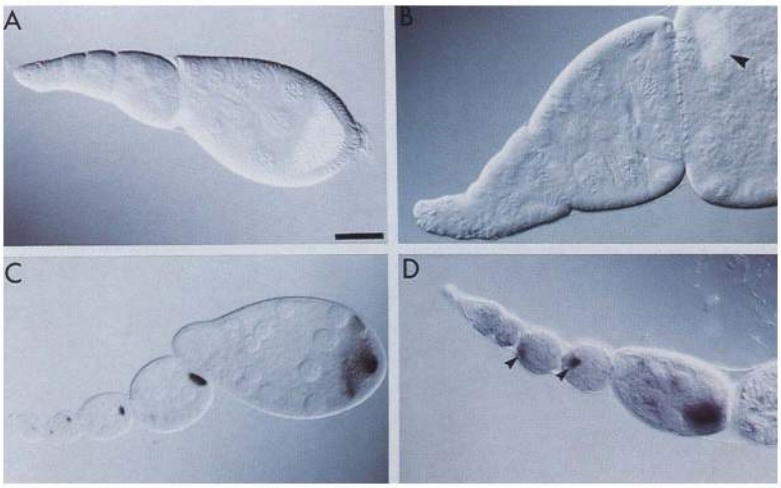

Figure 1. Egg chambers from *hls* females exhibit mispositioned oocytes. (*A*) Wild-type ovariole. The S9 egg chamber conrains an oocyte located at the posterior. (*B*) hls^{3987} ovariole. The S8 egg chamber contains a vitellogenic cell located at the anterior (arrowhead). (*C,D*) Ovarioles probed with *osk* cDNA sequences to identify previtellogenic oocytes (*C*) Wild type; (*D*) hls^{3987}. Arrowheads indicate two mispositioned oocytes. Bar in *A*, 20 μm. Note: We distinguish the mispositioned oocyte phenotype of *hls* egg chambers from that of *dicephalic* (*dic*) egg chambers. The term dicephalic implies the presence of nurse cells at each end of the developing egg chamber. In *hls* egg chambers in which the oocyte is not posteriorly positioned, the oocytes are fully anteriorly localized as frequently as they are centrally located. In addition, some *dic* eggs generate two micropyles. We have not observed bipolar chorion structures on eggs produced by *hls* females.

duced fewer late-stage egg chambers because of a higher number of eggs that degenerated at all stages (Table 1). These results suggested that the insertion line was a hypomorph. Two ethylmethane sulfonate (EMS)-induced alleles of *hls*, hls^{E616} and hls^{E653}, were kindly provided by Daniel St. Johnston (Wellcome/CRC Institute, Cambridge, UK). When placed in *trans* to a deficiency for the region, these lines were somewhat weaker than hls^{3987} hemizygotes (Tables 1 and 2), suggesting that these alleles are also hypomorphs.

To generate additional alleles for further study of the *hls* gene, we excised the P(*lacZ*,ry^+) element in hls^{3987} using the Δ2-3 transposase, scoring for loss of the *rosy*$^+$ (ry^+) eye color marker (Robertson et al. 1988). We hoped to obtain less severe lines in which eggs were laid and any embryonic defects might be analyzed, as well as stronger alleles in which the expressivity of the oogenesis phenotypes might be increased. Following two independent transposase-induced excision screens, 280 ry^- lines were established. Of these lines, 31% were fully fertile, demonstrating that the P element was responsible for the female sterile phenotype. The sterile, imprecise excision lines, however, were all similar to our starting allele in phenotype and range of expressivity. Molecular analyses demonstrated that the P element is inserted within the coding region of the gene (see below), and we speculate that the presence of any extraneous DNA is deleterious. We did recover three excision lines that fall into one lethal complementation group, are uncovered by a deficiency for the region, and are sterile in *trans* to the starting P allele. Two of these lines, $hls^{\Delta 157}$ and $hls^{\Delta 139}$, contain deletions of most or all of the P element and 1–2 kb of the *hls* gene 3′ to the P element insertion site (Fig. 3A). These lines therefore may be null for *hls* function. A third lethal line, $hls^{\Delta 125}$, contains a deletion of the P element and at least 6 kb 3′ to the P element insertion site, and thus may affect additional genes. Examination of the lethal phase of these deletion alleles demonstrated that $hls^{\Delta 125}$ homozygotes die as embryos, whereas $hls^{\Delta 157}$ and $hls^{\Delta 139}$ animals die at all stages of development.

Mutations in hls *affect oocyte localization and dorsal eggshell appendage formation*

Ovaries from hls^{3987}, hls^{3987}/Df, hls^{E616}/Df, and $hls^{E653}/$

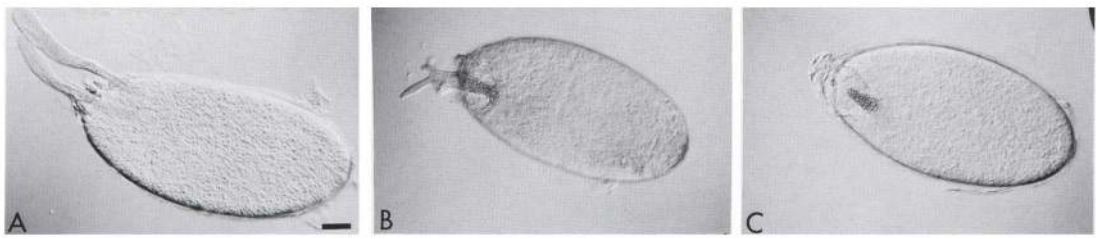

Figure 2. *hls* egg chambers show a range of ventralized phenotypes. Some wild-type chorion structures are observed, but no eggs hatch from homozygous *hls* females. The S14 egg chambers shown here were obrained from dissected ovaries, because few eggs are laid. (*A*) Wild-type S14 egg chamber showing the characteristic dorsolateral respiratory appendages. (*B*) hls^{3987} S14 egg chamber. The "forked" respiratory appendages arise from a single base on the midline. (*C*) A more ventralized hls^{3987} S14 egg with a single dorsal appendage. Bar in *A*, 20 μm.

Table 1. *Oocyte mislocalization and early degeneration*

Genotype	*n*	Mislocalized oocyte (%)[a]	Degenerating S8–S10 egg chamber (%)
hls^{3987}	123	6 (5)	7 (6)
	127	9 (7)[b]	—
hls^{3987}/*Df(3R)sbd*^{105}	100	11 (11)	38 (38)
hls^{E616}/*Df(3R)sbd*^{105}	125	7 (6)	21 (17)
hls^{E653}/*Df(3R)sbd*^{105}	163	7 (4)	21 (13)

[a]Based on vitellogenic egg chambers (S8–10)
[b]Based on *oskar* hybridization (S1–10)

Df females contained a small percentage of vitellogenic egg chambers with mislocalized oocytes (Fig. 1B; Table 1). To quantify mislocalization in previtellogenic egg chambers, we identified the oocyte by detecting the presence of *osk* transcripts, which are produced in the nurse cells and then transported to the oocyte early in oogenesis (Fig. 1C; Ephrussi et al. 1991; Kim-Ha et al. 1991). The *osk* probe recognized transcripts in a single germline cell in *hls* egg chambers (Fig. 1D). In some egg chambers, the labelled cell was not the posterior-most cell, indicating a mispositioned oocyte (Fig. 1D, arrowheads). In *hls*^{3987} homozygotes, 7% of S1–S10 egg chambers contained mislocalized oocytes (Table 1).

Ovaries dissected from *hls*^{3987} females also contained a range of late-stage phenotypes (Table 2). A wild-type egg chamber at S14 possesses two dorsal eggshell respiratory appendages, just lateral to the dorsal midline (Fig. 2A). Some wild-type-appearing egg chambers were recovered from *hls*^{3987} females, but 90%–95% of the egg chambers showed aberrant appendage formation; the majority possessed only one appendage or fused appendages emerging from one base on the dorsal midline (Fig. 2B,C; Table 2). Females transheterozygous for either *hls*^{E616} or *hls*^{E653} and *Df(3R)sbd*^{105} produced egg chambers with a similar range of phenotypes (Table 2).

Cloning of the hls *gene*

To characterize the *hls* gene at the molecular level, DNA flanking the 5′ end of the P element was cloned by screening a λ library of *hls*^{3987} DNA with a probe complementary to the P element 5′ end. The 1.5 kb of flanking DNA obtained in this way was used to isolate two cosmids from a *cosPneo* library (gift of Mark Champe, Genentech, San Francisco, CA) (Fig. 3A). In addition, the 1.5-kb flanking DNA hybridized to two abundant transcripts on a Northern blot of wild-type female RNA. A 1.1-kb transcript showed no variation in length or expression levels between wild-type and *hls*^{3987} females (data not shown). Partial sequence of genomic DNA encoding the 1.1-kb transcript revealed strong homology (84% identity) to bovine NADH dehydrogenase (H. Enderlin, D. Gillespie, and C. Berg, unpubl.). A second, 4.6-kb transcript was abundant in wild-type females but nearly absent in *hls*^{3987} females. We refer to the 4.6-kb transcript as the *hls* transcript. A subclone specific to the *hls* transcript was used to isolate a 4.6-kb cDNA from an ovarian cDNA library (Stroumbakis et al. 1994). When this cDNA was used as a probe against Northern blots (Fig. 3B), it recognized the same 4.6-kb transcript as well as an additional, much less abundant, 11-kb transcript whose expression pattern paralleled that of the *hls* transcript. This additional message may represent either a pre-mRNA for the *hls* transcript or an alternatively spliced message. Both the 4.6- and 11-kb transcripts were expressed primarily in ovarian tissue, although small amounts were detected in total male and in female carcass RNA. The cDNA also hybridized to a rare, 9-kb transcript, expressed at extremely low levels in ovaries and at moderate levels in male and female carcass tissues. This transcript was unaffected by the P element

Table 2. *S14 respiratory appendage formation in* hls *ovaries*

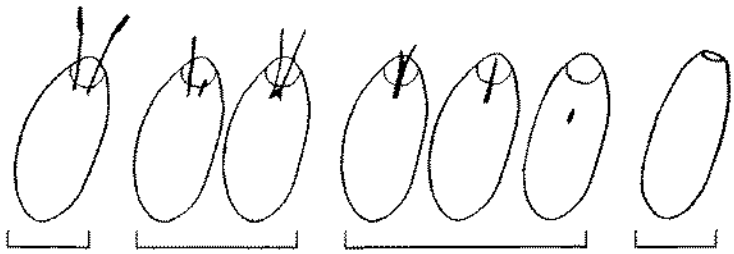

Genotype					
3987/3987	n=	28	69	305	60
	(%)	(6)	(15)	(66)	(13)
E616/Df	n=	0	0	55	40
	(%)			(58)	(42)
E653/Df[a]	n=	1	9	52	51
	(%)	(1)	(8)	(46)	(45)

Numbers are from ovaries dissected from 2 to 5-day-old females.
[a]We also observed variable cup and dumpless phenotypes in some females dissected from this genotype.

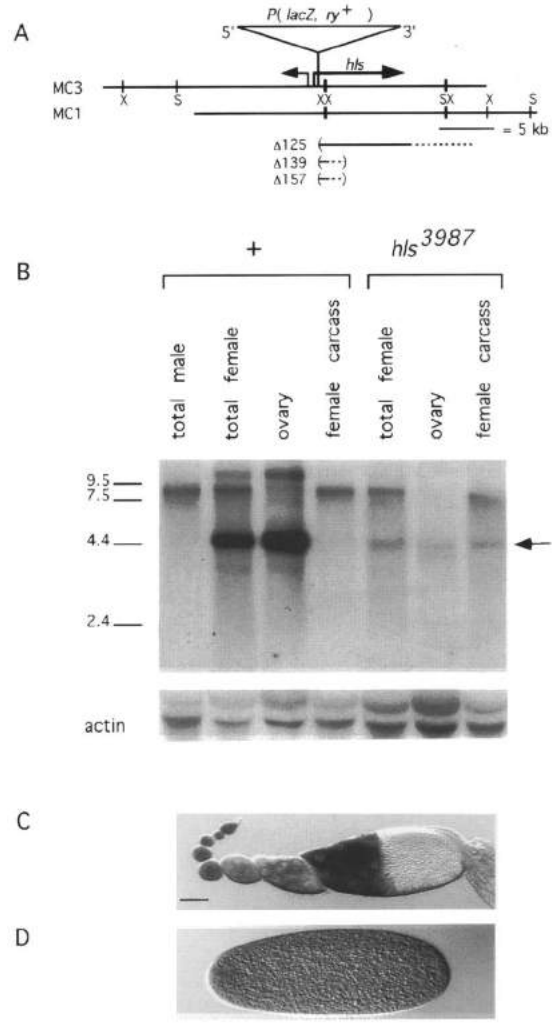

Figure 3. (*A*) Molecular map of the *hls* locus. Cosmids MC1 and MC3 were isolated by using a probe from DNA flanking the 5′ end of the *P* element (see text). The 4.6-kb *hls* transcript is indicated as the large arrow pointing to the *right*. The smaller arrow pointing to the *left* represents a transcript encoding a protein highly homologous to NADH dehydrogenase. The deletions present in $hls^{\Delta 125}$, $hls^{\Delta 139}$, and $hls^{\Delta 157}$ are shown below the map as thin lines bounded by parentheses. The solid lines indicate DNA that is known to be deleted; dotted lines indicate DNA that may be deleted. (X) *Xba*I; (S) *Sal*I. (*B*) Northern blot probed with the 4.6-kb *hls* cDNA (cD5). Total RNAs (35 μg) were loaded in each lane. The 4.6-kb *hls* transcript (arrow) is expressed predominantly in females and is enriched in ovarian RNA. This transcript is nearly absent in RNA from hls^{3987} homozygous females. (*C*) The same blot was stripped and reprobed to identify *actin* mRNA as a control to show the amount of RNA present in each lane. (*C,D*) In situ hybridization of wild-type tissue using the *hls* cDNA as a probe. (*C*) Ovariole, germarium through S10. The transcript is first detected in the germarium, falling off in the nurse cells through S4–S5, then increasing in S8, and strongest in S10. The message is transported into the oocyte during S11 and is not localized within the embryo. (*D*) Preblastoderm stage embryo. Bar in *C*, 20 μm.

insertion (Fig. 3B). The lethality of the deletion alleles could be attributable to the lack of carcass transcripts.

To determine the spatial pattern of *hls* expression, digoxigenin-labeled cDNA sequences were used to probe wild-type ovaries by in situ hybridization. In the germarium, hybridization appeared to be limited to the germline cells (Fig. 3D). *hls* expression decreased through S4/S5, increased during S8, and was strongest in the nurse cells at S10 (Fig. 3D). No transcript was detected in the oocyte until S11, when the nurse cell contents are deposited into the oocyte. The *hls* transcript was distributed uniformly in the early embryo (Fig. 3E).

hls *encodes a putative member of the DE-H family of RNA-dependent ATPases/helicases*

The sequence of the *hls* cDNA (Fig. 4) indicated a coding region of 4377 nucleotides, predicting a protein of 1459 amino acids having a molecular mass of ~155 kD. The carboxy-terminal two-thirds of the predicted protein revealed no homology in searches using the BLAST and GCG programs. The amino-terminal sequence, however, contained a region similar to yeast splicing factors PRP2 (pre-mRNA processing protein-2) (Chen and Lin 1990) and PRP16 (Burgess et al. 1990) and to the *Drosophila* Maleless (Mle) protein, which is required for dosage compensation (Kuroda et al. 1991) (underlined region in Fig. 4; Fig. 5). These proteins are members of a large superfamily of RNA-dependent ATPases and helicases, which contain seven broadly defined domains (Hodgman 1988). Within these seven domains, Hls shares ~29% identity and 51% similarity with PRP2, PRP16, and Mle. As indicated in Figure 5, domain I contains an ATP/GTP-binding motif.

Hls *plays a role in localizing RNAs*

The similarity to proteins that function through binding RNAs suggested a possible role for Hls in RNA processing, transport, or stabilization. Therefore, we examined the localization patterns of seven previously characterized mRNAs that are known to be localized during oogenesis. Our work placed these transcripts into three classes: (1) those that failed to be transported or localized correctly in some fraction of *hls* egg chambers, (2) those that were localized correctly but were reduced in amount, and (3) those unaffected in *hls* mutants.

The first class of messages was identified by examination of the localization patterns of the *grk*, *osk*, and *bcd* mRNAs. Because of the highly penetrant dorsoventral defects in late-stage *hls* egg chambers, we suspected that *grk* expression or localization might be defective. In wild-type oocytes, the *grk* transcript is tightly localized to the dorsal anterior cortex, overlying the nucleus in a cap at S9 and S10 (Fig. 6A; Neuman-Silberberg and Schüpbach 1993). Surprisingly, we found that *grk* mRNA was localized appropriately in the majority of S9 and S10 *hls* egg chambers (Fig. 6B; Table 3). In ~30% ($n=52$) of *hls* egg chambers, however, the pattern was defective. We observed some eggs with no *grk* mRNA localization, some S10 eggs with an anterior ring (Fig. 6C), and some

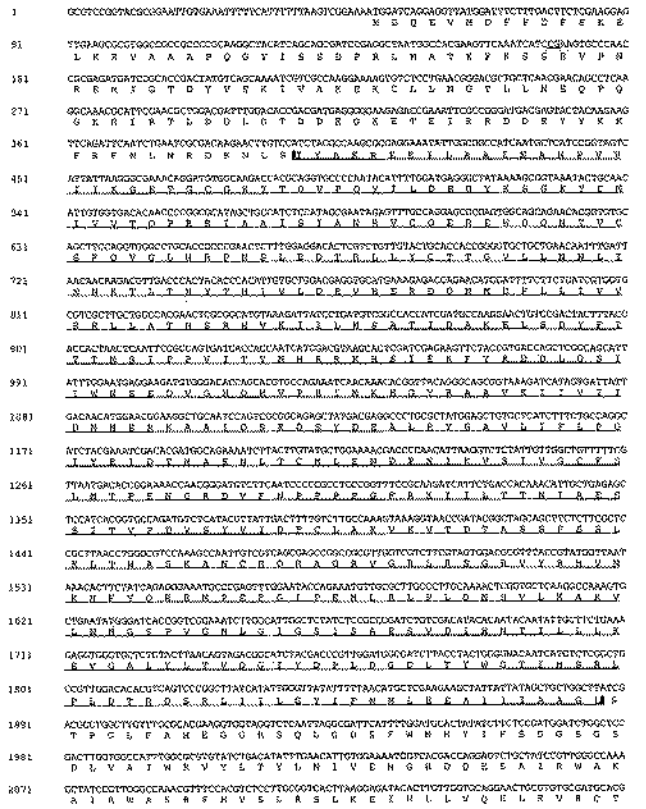

Figure 4. cDNA sequence and predicted protein sequence of *hls* cDNA. The sequence presented here was generated from a single, full-length cDNA (cD5). The numbers correspond to DNA base sequence. The region aligned for homology comparison in Fig. 5 is underlined. The 2 bases between which the P element is inserted in *hls*^{3987} (nucleotides 168 and 169) are underlined.

with a dorsal patch that was broader than normal (Table 3).

As described above, we used in situ hybridization with an *osk* cDNA probe to identify the previtellogenic oocytes in *hls* ovaries. Although *osk* RNA was transported to the oocyte normally in these early stages, later localization to the posterior pole was defective. In the majority of S10 egg chambers, *osk* RNA was diffuse throughout the oocyte (Fig. 6E). In those egg chambers in which *osk* RNA was not distributed uniformly, only 12% ($n = 77$) contained *osk* message correctly localized to the posterior pole. More frequently, we observed a diffuse accumulation of *osk* RNA in the center or toward the anterior of the oocyte (Fig. 6F; Table 3). About half of the eggs within this latter class also had a small amount of *osk* mRNA localized to the posterior pole (Fig. 6F).

Bcd is an anterior determinant whose transcript is lo-

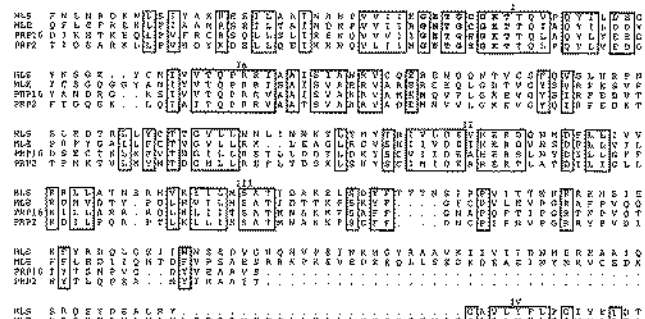

Figure 5. Alignment of the amino-terminal region of Hls with three DE-H family members. Hls amino acids 116–623 are aligned with *Drosophila* Mle and yeast PRP2 and PRP16. Identical and similar amino acids are boxed if represented in all four proteins. Acceptable similarities were as follows: [V,I,L,M]; [F,Y,W]; [R,K]; [D,E]; [T,S]. Roman numerals indicate the seven motifs originally identified by Hodgman (1988) and found in the DEAD/DE-H superfamily. No definitive consensus sequences or boundaries for each motif have been described in the literature. The ATP/GTP-binding domain is indicated in bold.

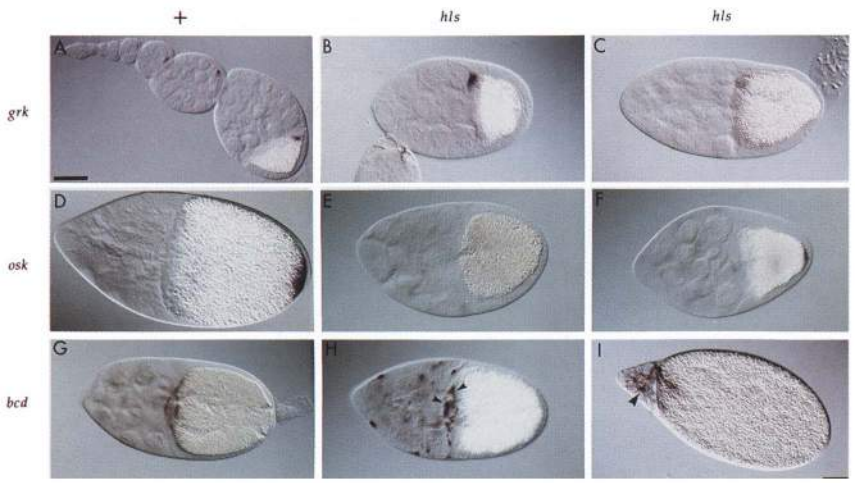

Figure 6. Wild-type and hls^{3987} egg chambers, probed with *grk*, *osk*, and *bcd* sequences. (*A*) Wild-type ovariole, probed with *grk* sequences. (*B,C*) hls^{3987} egg chambers, probed with *grk* sequences. *grk* message is localized correctly in the majority of S10 *hls* egg chambers (*B*), but in some S10 egg chambers, *grk* transcript is absent or localized in a faint anterior ring (*C*). (*D*) S10 wild-type egg chamber, probed with *osk* sequences. (*E,F*) hls^{3987} egg chambers, probed with *osk* sequences. In the majority of S10 *hls* egg chambers (*E*), *osk* message is diffuse throughout the oocyte. Occasionally, *osk* mRNA accumulates near the anterior or in the center of the oocyte, frequently coupled with a small amount of *osk* transcript at the posterior pole, shown here (*F*) in a S9 egg chamber. (*G*) S10 wild-type egg chamber, probed with *bcd* sequences. (*H,I*) hls^{3987} egg chambers, probed with *bcd* sequences. *bcd* message is detected in a punctate pattern in S10 *hls* egg chambers, and the majority of the message is retained in the nurse cells (*H*). Arrowheads (*H*) mark clusters of *bcd* transcript that fail to move laterally to the outer cortex. In S11 wild-type egg chambers, no *bcd* transcript is detected in the nurse cells (data not shown), whereas nurse cells in S11 *hls* egg chambers (*I*) retain significant amounts of *bcd* message (arrowhead). The bar in *A* applies to *A–H* and is 20 μm; Bar in *I*, also 20 μm.

calized to the anterior cortex of the oocyte during S8–S10 of oogenesis (Fig. 6G; Berleth et al. 1988; St. Johnston et al. 1989). The mRNA is produced in the nurse cells where it transiently accumulates at the apical cortex before being transported to the oocyte (Berleth et al. 1988; St. Johnston et al. 1989). In *hls* egg chambers, we observed clearly aberrant *bcd* mRNA distribution in S8. In most egg chambers (Fig. 6H; Table 3), some *bcd* message was transported to the oocyte, but the majority remained in the nurse cells, concentrated at the apical cortex. In addition, much of the *bcd* message within the oocyte was not transported laterally toward the periphery but instead remained centrally located, possibly at the site of the ring canals that connect the nurse cells to the oocyte (Fig. 6H, arrowheads). Even during the normal bulk transport of material from the nurse cells to the oocyte at S11, some *bcd* message still remained in the nurse cells (Fig. 6I, arrowhead). The failure to transport *bcd* mRNA to the oocyte and *osk* message within the oocyte during S8–S10 are the earliest defects in RNA transport we observe in *hls* mutants and clearly indicate that normal *hls* functions are disrupted at the beginning of vitellogenesis.

Examination of two other anteriorly localized tran-

Table 3. *Localization of mRNAs in S10 egg chambers*

mRNA	Wild type	hls^{3987}	Percent egg chambers[a]
gurken	dorsal anterior	dorsal anterior	68
		broader dorsal patch	14
		anterior ring	13
		no localization	5
oskar	posterior pole	posterior pole	12
		anterior or central cloud, plus some at posterior	14
		anterior or central cloud only	14
		diffuse throughout the oocyte	60
bicoid	anterior cortex	majority at anterior of oocyte, plus some in nurse cells	10
		clumps at anterior of oocyte and punctate in nurse cells	74
		none in oocyte and punctate in nurse cells	16
K10	anterior	anterior, reduced amount	100[b]
orb	anterior	anterior, reduced amount	100[b]
Bicaudal-D	anterior cortex	anterior cortex	100
hu-li tai shao	anterior cortex	anterior cortex	100

The localization patterns in previtellogenic stages were similar in wild-type and *hls* egg chambers for all transcripts listed.
[a]*gurken*, $n = 52$; *oskar*, $n = 77$; *bicoid*, $n = 49$; *k10*, $n = 50$; *orb*, $n = 79$; *Bicaudal-D*, $n = 127$; *hu-li tai shao*, $n = 42$.
[b]Although proper localization was observed in 100% of egg chambers, transcript levels were reduced.

scripts, the *K10* and *orb* mRNAs, identified a second class of messages. *K10*, which is required for correct *grk* mRNA localization and dorsoventral axis formation (Wieschaus et al. 1978; Neuman-Silberberg and Schüpbach 1993), is transcribed in the nurse cells. The message is transported to the oocyte during previtellogenic stages (Cheung et al. 1992; Fig. 7A). At the onset of vitellogenesis (S8), the transcripts are localized to the anterior edge of the oocyte where they accumulate through S10 (Fig. 7B). In a hls^{3987} background, *K10* transcripts were transported to the oocyte and later localized to the anterior edge (Fig. 7C), but the level of transcript was greatly decreased relative to wild type, specifically in vitellogenic stages (Fig. 7D).

Our observations using an *orb* cDNA probe were similar to those with *K10*. The *orb* gene encodes sex-specific RNA-binding proteins (Lantz et al. 1992) required for correct *osk* and *grk* mRNA localization (Christerson and McKearin 1994). In wild-type ovarioles, *orb* transcript is transported to the oocyte in the germarium and continues to accumulate in the oocyte through previtellogenic stages (Fig. 7E). At S8, the transcript is localized to the anterior edge of the oocyte, but unlike *K10*, the intensity of the anterior band decreases through S10 (Fig 7F; Lantz et al. 1992). In hls^{3987} egg chambers, *orb* mRNA accumulated normally in the oocytes of early egg chambers (Fig. 7G), but the anterior localization, while present, was significantly weaker in S8–S10 (Fig. 7H).

We found that the transport and localization patterns of the *Bic-D* and *hts* mRNAs did not change in hls^{3987} ovaries. Following early oocyte accumulation, the *Bic-D* transcript is localized to the anterior of the oocyte at S8 (Fig. 7I). This anterior localization is maintained through S10, at which time nurse cell expression of *Bic-D* increases dramatically (Fig. 7J; Suter et al. 1989). *hts* transcripts are also present in low levels in wild-type germaria and are transported to the oocyte from the nurse cells (Yue and Spradling 1992; Ding et al. 1993b). During vitellogenic stages, *hts* transcripts are localized predominantly to the anterior of the oocyte (Fig. 7M) and remain localized during nurse cell dumping at S11 (Fig. 7N).

Figure 7. Wild-type and hls^{3987} egg chambers, probed with *K10*, *orb*, *Bic-D*, and *hts* sequences. (*A,B*) Wild-type egg chambers, probed with *K10* sequences. (*C,D*) hls^{3987} egg chambers, probed with *K10* sequences. Localization of *K10* message to the oocyte is normal during early oogenesis (*C*). Anterior localization of *K10* transcript occurs normally in S10 *hls* egg chambers (*D*), although the amount is reduced (*D*) compared to wild type (*B*). (*E,F*) Wild-type egg chambers, probed with *orb* sequences. (*G,H*) hls^{3987} egg chambers, probed with *orb* sequences. *orb* message is transported normally to the oocyte in *hls* egg chambers during early oogenesis (*G*). Anterior localization is normal in S10 *hls* egg chambers, but the level is reduced (*H*). (*I,J*) Wild-type egg chambers, probed with *Bic-D* sequences. (*K,L*) hls^{3987} egg chambers, probed with *Bic-D* sequences. Early transport to the oocyte and anterior localization within the oocyte is observed in both wild-type (*I*) and *hls* (*K*) ovarioles. Transcription of *Bic-D* increases dramatically during S9 and S10, and message within the oocyte is anteriorly localized in both wild-type (*J*) and *hls* egg chambers (*L*). (*M,N*) Wild-type egg chambers, probed with *hts* sequences. (*O,P*) hls^{3987} egg chambers, probed with *hts* sequences. Localization of *hts* message during all stages of oogenesis (*O,P*) is normal in *hls* egg chambers. Bar in *A*, 20 μm.

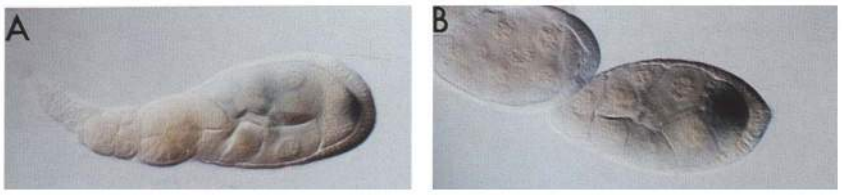

Figure 8. Kin:β-Gal localization in wild-type and *hls* egg chambers. (*A*) S8 wild-type egg chamber. At S8, Kinesin-directed β-Galactosidase activity is observed at the posterior of the oocyte. (*B*) S8 hls^{3987} egg chamber. β-Gal activity indicates that the fusion protein is diffuse throughout most of the oocyte.

These patterns were not affected by our hls^{3987} mutation (Fig. 7K,L,O,P).

Microtubule structure is disrupted in hls *egg chambers*

Because the Hls protein has homology to RNA-binding proteins of the DE-H family, it seemed likely that it was acting directly to localize RNAs in oogenesis. It was possible, however, that mutations in the gene were affecting RNA localization by disrupting the microtubule architecture that is a common component of the localization mechanisms of these RNAs (Koch and Spitzer 1983; Pokrywka and Stephenson 1991, 1995; Theurkauf et al. 1993; for review, see Theurkauf 1994a). In addition, the diffuse *osk* mRNA pattern that we observed in *hls* egg chambers has been described in mutants affecting microtubule organization (Ephrussi et al. 1991; Kim-Ha et al. 1991; Ruohola et al. 1991; Clark et al. 1994; González-Reyes and St. Johnston 1994; Lane and Kalderon 1994; Theurkauf 1994b; González-Reyes et al. 1995; Roth et al. 1995). Hence, we examined the localization of a Kinesin heavy chain:β-Galactosidase (Kin:β-Gal) fusion protein (Clark et al. 1994) in a hls^{3987} background to analyze one aspect of microtubule structure and function. In wild-type S8 and S9 egg chambers, microtubule organizing centers (MTOCs) are located at the anterior of the oocyte and direct the formation of a gradient of microtubules whose plus ends extend toward the posterior pole (Theurkauf et al. 1992). The fusion protein is thus propelled by the plus-end-directed kinesin motor function and is present in a band at the posterior of the oocyte, as detected by β-Galactosidase activity on an X-Gal substrate (Fig. 8A). In a *hls* background, we detected the fusion protein in the center of S8 oocytes and in the central and lateral portions of S9 oocytes (Fig. 8B), suggesting that microtubule structure or function is disrupted.

To verify our results using the Kin:β-Gal fusion protein, we directly examined microtubule organization in *hls* egg chambers by comparing anti-α-Tubulin immunofluorescence in wild-type and hls^{3987} ovaries. An accumulation of microtubules, indicating the MTOC, is observed at the posterior of the oocyte prior to vitellogenesis in wild-type egg chambers (Fig. 9A; Theurkauf et al. 1992). At the onset of vitellogenesis in S8, the MTOC is no longer present at the posterior, having moved anteriorly along the cortex (Fig. 9C,E). This anterior cortical accumulation is still apparent during S9 (Fig. 9G) and persists through S10a. The oocyte nucleus moves anteriorly with the MTOC at S8 (Theurkauf et al. 1992). In *hls* egg

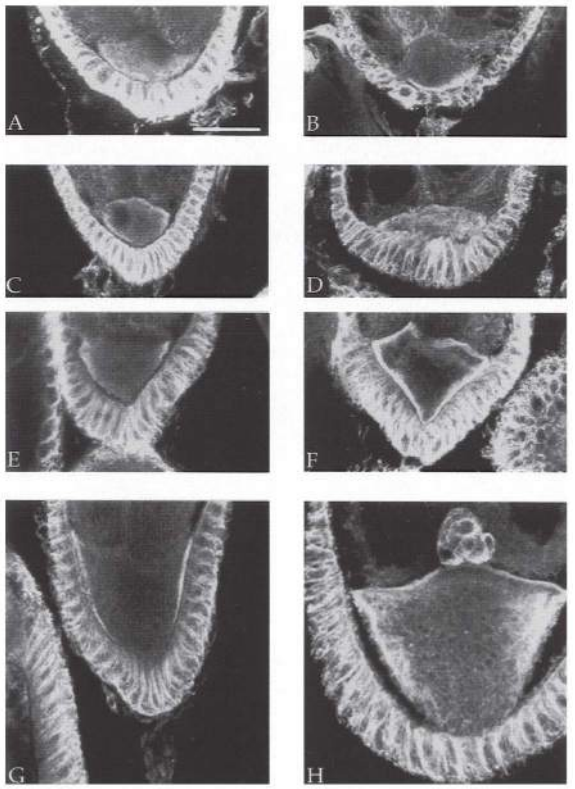

Figure 9. Microtubule organization in wild-type and hls^{3987} egg chambers. We visualized microtubule structure by immunofluorescence using anti-α-Tubulin antibodies. Each image is a projection of three confocal images, 1 μm apart. Posterior is toward the *bottom*. (*A,C,E,G*) Wild-type oocytes; (*B,D,F,H*) hls^{3987} oocytes. In S7 oocytes from wild-type (*A*) and *hls* (*B*) egg chambers, we observed similar posterior accumulation of microtubules. Cortical microtubules move anteriorly in early wild-type S8 oocytes (*C*) and are absent at the posterior by late S8 (*E*). Two main phenotypes were observed in *hls* egg chambers. Over half of *hls* S8 oocytes contained long internal microtubule bundles (*D*); in the remaining oocytes, cortical accumulation was present at the anterior but also persisted at the posterior (*F*). In wild-type S9 oocytes, little or no internal microtubule meshwork was detected (*G*), whereas *hls* S9 oocytes contained extensive microtubules initiating at the cortices and extending into the cytoplasm centrally and posteriorly (*H*). This image also illustrates the premature arrival of the border cells at the nurse cell/oocyte boundary. The membrane separation observed in this image was a result of dehydration during methanol fixation and was observed in both wild-type and *hls* egg chambers.

chambers, we observed a normal posterior concentration of microtubules prior to vitellogenesis (Fig. 9B). In contrast, a dense network of microtubules was present throughout the oocyte in 64% ($n = 55$) of the S8 *hls* egg chambers (Fig. 9D). In the remainder of the S8 egg chambers, cortical microtubule accumulation was observed both posteriorly and anteriorly (Fig. 9F). *hls* S9 egg chambers contained an extensive microtubule mesh concentrated at the anterior cortices (72%, $n = 14$). Unlike wild type, this mesh clearly extended centrally and posteriorly into the cytoplasm. In all cases, the oocyte nucleus was correctly positioned at the dorsal anterior corner of the oocyte.

During S10b, the oocyte microtubules reorganize and begin cytoplasmic streaming in preparation for the transport of cytoplasm from the nurse cells (Gutzeit and Koppa 1982; Theurkauf et al. 1992). Despite the presence of an aberrant network in S8–S9 *hls* egg chambers, we observed normal microtubule rearrangements in S10b *hls* oocytes (data not shown). Time-lapse photography also indicated that temporal regulation of streaming in *hls* egg chambers is identical to that in wild type (data not shown). Thus, the observed defects in RNA and Kin:β-Gal localization in *hls* egg chambers are not attributable to premature cytoplasmic streaming but, rather, to the inappropriate formation of an extensive microtubule meshwork during S8–S9.

Discussion

The *hls* gene is required for proper localization of several RNAs that are involved in anteroposterior and dorsoventral axis formation during oogenesis. Based on the RNA localization patterns and microtubule structure in *hls* mutants, and the similarity of Hls protein to members of the DE-H family of RNA-binding proteins, we present models for the role of Hls in oogenesis.

Hls contains homology to RNA-dependent ATPases

Sequence analysis revealed that the predicted amino-terminal region of the Hls protein is similar to the DE-H family of RNA-dependent ATPases. Although literature citations frequently refer to members of this family as helicases, only some DE-H proteins have demonstrated helicase activity. For example, human RNA Helicase A and vaccinia virus NPH-II have exhibited the ability to unwind double-stranded RNA (Shuman 1992; Lee and Hurwitz 1993). In contrast, two of the three proteins that share strong similarity with Hls, PRP2 and PRP16, demonstrated no helicase activity when tested (Schwer and Guthrie 1991; Kim et al. 1992). The third protein, Mle, has not been examined, although it contains extensive identity over its entire length to the known helicase human RNA Helicase A. Interestingly, Mle and Hls share a similar structure in that their homologous domains are limited to the amino-terminal third of the proteins. In PRP2, an 876-amino-acid protein, the DEAD/DE-H domain is located centrally in the sequence, similar to the structure of the 1071-amino-acid PRP16.

PRP2 and PRP16 both exhibit nonspecific RNA-binding activity and hydrolyze ATP when single-stranded RNA is provided (Schwer and Guthrie 1991; Kim et al. 1992). PRP2 is required for the 5′ cleavage reaction in splicing (Kim and Lin 1993), and PRP16 for 3′ cleavage (Schwer and Guthrie 1991). Mle is implicated in dosage compensation in *Drosophila* (Belote and Lucchesi 1980) and binds predominantly to the X chromosome in males (Kuroda et al. 1991). The identity of the bound substrates and any biochemical activities of Mle have not been established. Kuroda et al. (1991) propose models in which Mle is involved in transcript elongation, release of the nascent RNA from the template, or increasing RNA processing efficiencies.

Vasa, a member of the DEAD/DE-H superfamily (Lasko and Ashburner 1988), is required to establish a/p polarity during *Drosophila* oogenesis. This DEAD-box protein is necessary for the localization of *nanos* transcripts to the posterior pole during oogenesis. Hls is the first member of the DE-H-box family implicated in RNA transport and localization. Whereas the sequence similarity suggests that Hls interacts directly with RNA molecules, the defects in cytoskeletal organization argue that Hls functions indirectly in localizing specific RNAs required for embryonic polarity. How does *hls* fit in to the known pathways required for RNA localization?

hls *is unique among patterning mutants*

Over the last two decades, a large number of genes required during *Drosophila* oogenesis for proper localization of RNAs involved in a/p or d/v patterning have been identified. In addition, the dynamic patterns of cytoskeletal organization have been characterized, and requirements for various cytoskeletal components in axis formation have been defined. The *hls* gene appears to be a link between patterning genes and microtubule architecture.

The mispositioned oocyte and ventralized late-stage egg chamber phenotypes of *hls* ovaries bear a striking resemblance to some defects observed in members of the spindle class of maternal effect mutants (Tearle and Nüsslein-Volhard 1987). In *spn-C* mutants, for example, Kin:β-Gal movement and the localization of some RNAs are disrupted in dicephalic egg chambers, but not in *spn-C* egg chambers in which the oocyte is positioned normally at the posterior of the egg chamber (González-Reyes and St. Johnston 1994). These results suggest that the positioning of the oocyte within the egg chamber directs the formation of the microtubule network within the egg and in this way affects the localization of both RNA and protein products. *hls* differs from these mutants in that Kin:β-Gal and the various RNAs are also mislocalized in egg chambers of normal polarity.

The female sterile genes *cappucino* and *spire* are thought to regulate the microtubule-dependent cytoplasmic streaming that occurs in S10B–S12 oocytes (Theurkauf 1994b). Mutations in these genes result in the mislocalization of several RNAs and proteins, including *osk*, *K10*, and *grk* mRNAs and Kin:β-Gal and Stau proteins (Ephrussi et al. 1991; Kim-Ha et al. 1991; St. Johnston et

al. 1991; Cheung et al. 1992; Neuman-Silberberg and Schüpbach 1993; Clark et al. 1994). Although these mutants are similar to *hls* in their variability and range of phenotypes, cytoplasmic streaming initiates normally in *hls* egg chambers. In addition, *cappucino* and *spire* differ from *hls* in that they do not disrupt localization of *bcd* mRNA in the nurse cells or in the oocyte.

The phenotypes of *hls* mutants most closely resemble those observed in *Notch* (*N*), *protein kinase A* (*PKA*), *grk*, *top*, and *cni* mutants (Ruohola et al. 1991; Lane and Kalderon 1994; González-Reyes et al. 1995; Roth et al. 1995). Mutations in these genes also affect microtubule structures, but in these cases by disrupting signal transduction pathways required for normal microtubule reorganization within the oocyte during S7–S9. In egg chambers from these mutants, Kin:β-Gal is centrally located in the oocyte, suggesting that microtubules are organized with their positive ends toward the center. *osk* RNA is also found in the center, whereas *bcd* message appears at both anterior and posterior poles. Although Hls may be required in these pathways to direct the microtubule changes that occur during mid-oogenesis, it must also play an additional role in *bcd* mRNA transport from nurse cells to oocyte. Unlike the observations made with *N*, *PKA*, *grk*, *top*, and *cni* mutants, *bcd* message is never detected at the posterior of *hls* egg chambers, even in those few egg chambers in which *bcd* mRNA is present in the oocyte. The retention of *bcd* message in nurse cells is not due to a failure in general transport, as the bulk of nurse cell cytoplasm flows normally into the oocyte at S11. Thus, the *bcd* transcript must be retained because of a specific defect in cytoskeletal architecture or the absence of some critical component in the transport process.

Models for hls *function*

From our analyses, we conclude that mutations in *hls* disrupt microtubule organization at the onset of vitellogenesis, subsequently affecting the transport and localization of selected mRNAs. The expression of *hls* during early oogenesis, the early phenotype of mislocalized oocytes, and the subsequent degeneration during all stages indicate that Hls also functions during early stages. Construction of germ-line clones with lethal excision lines may enhance the penetrance of the early defects and reveal an essential requirement for Hls in previtellogenic egg chambers, perhaps in oocyte specification, microtubule organization, or transport of transcripts to the oocyte. The strong mutant phenotypes observed in the hypomorphic alleles suggest that Hls acts predominantly during vitellogenic stages, and this study has focused on the role of *hls* during those stages.

We postulate that Hls could be functioning in one of two ways. First, Hls could act downstream of the signaling pathways that induce correct microtubule reorganization during S8 and S9, actively interacting in microtubule reorganization. A second possibility is that Hls is required for efficient transcription, pre-mRNA processing, localization, or translational regulation of products that control the kinetics of microtubule assembly or direct the reorganization of microtubule structures. The similarity of Hls protein to members of the DE-H family makes this hypothesis attractive.

To determine the function of *hls* in axis formation during oogenesis, we examined the distribution of seven different mRNAs in *hls* ovaries. These analyses coupled with observations of microtubule structures permit categorization of these transcripts by their dependence on properly organized microtubules for localization within the oocyte. Transport of *osk* and *bcd* RNAs is highly dependent on a well-organized, polarized network of microtubule arrays interconnecting the nurse cells and oocyte. We observed defective microtubule organization in 78% of *hls* S8 and S9 egg chambers, concomitant with mislocalized *osk* message in 88% of *hls* S8–S10 egg chambers. *bcd* mRNA was affected to a similar degree, with 90% of *hls* egg chambers exhibiting significant nurse cell retention of message. Defects in *bcd* message transport such as those we observe in *hls* mutants have not been described previously. Our data suggest that microtubule structures undergo a dynamic reorganization in nurse cells during S8, similar to that observed in the oocyte. In *hls* egg chambers, a lack of reorganization in the nurse cells could result in the abnormal retention of *bcd* mRNA at the nurse cells cortices.

Despite the severe microtubule defects observed in *hls* oocytes, the majority of *grk* mRNA is localized appropriately, presumably reflecting the correct positioning of the oocyte nucleus. The ventralization of *hls* egg chambers may be attributable to slightly lower levels of *grk* message (which we observed but is difficult to quantify), a defect in *grk* mRNA translation, or to the mislocalization or absence of an as-yet-unidentified transcript or protein. In addition, only a portion of the *K10* and *orb* messages are either mislocalized or degraded in *hls* oocytes, suggesting that microtubules are moderately necessary for their localization or stabilization at the anterior cortex. In contrast, *Bic-D* and *hts* transcripts are independent of the effect of *hls* mutations on microtubules, being correctly localized in *hls* egg chambers. These RNAs may be transported and localized when only a subset of the microtubule network is properly formed.

Transport and localization of *bcd*, *osk*, *Bic-D*, *orb*, and *K10* mRNAs have been well studied in ovaries treated with colchicine (Pokrywka and Stephenson 1991, 1995). Whereas all of these transcripts are vulnerable to microtubule depolymerization, their dependence on the exact polarization and organization of the cytoskeleton is not well demonstrated by such experiments. Drug treatment data, along with analyses of mutants such as *hls*, *N*, and *PKA*, will be necessary to understand fully the microtubule-mediated movement of mRNAs during oogenesis.

These studies provide the first evidence for a DE-H family member acting in processes that direct microtubule organization. Further characterization of the selective effects of *hls* mutations on specific transcripts will illuminate the different mechanisms for RNA localization and will clarify their relative dependence on the cytoskeleton.

Materials and methods

Fly stocks

The wild-type strain employed in our studies was Canton-S. hls^{E616} and hls^{E453}, generous gifts of Daniel St. Johnston, are listed in the Tübingen Stock List as *spindle-E* mutations (Tearle and Nüsslein-Volhard 1987). $Df(3R)sbd^{105}$ [88F9-89A1; 89B4-5] was described in Lindsley and Zimm (1992) and was obtained from the Bloomington Stock Center. Jim Kennison (National Institutes of Health, Bethesda, MD) provided additional deficiencies, $Df(3R)PO^{2-4}$, $Df(3R)c3G2$, $Df(3R)sbd^{26}$, and $Df(3R)sbd^{45}$, which were used for more precise mapping of the P element insertion site. *Kinesin heavy chain:lacZ* insertion line KL32, kindly provided by H. Ruohola-Baker (University of Washington, Seattle), was used for the Kin:β-Gal fusion protein studies. Fly stocks were maintained at 24°C on standard cornmeal/yeast/molasses medium.

To generate additional alleles of the *hls* gene, chromosomes carrying the P element insertion were first cleaned of potential background mutations in a process that recombined on the visible body color marker *ebony* (*e*). Excision lines then were generated by reintroducing the Δ2-3 transposase (Robertson et al. 1988). Males carrying both transposons were mated in vials to ry^{506} virgins, and the progeny were scored for loss of the ry^+ eye-color marker. ry^- F_1 males (280) were mated individually to $ry^{506}/TM3$, ry^{RK} *Sb* e^s virgin females to generate balanced stocks. Flies from each line were crossed to $hls^{3987}/TM3$ and $Df(3R)sbd^{105}/LVM$ flies to test viability and fertility.

Staining and in situ hybridization procedures

For β-Gal staining, ovaries were fixed and stained as described by Clark et al. (1994), except that the ovaries were fixed in 0.5% glutaraldehyde. Micrographs were generated on a Nikon Microphot FXA microscope using differential interference contrast optics.

For in situ hybridization to ovaries, a protocol adapted from Ephrussi et al. (1991) was used. Ovaries were dissected in modified EBR (129 mM NaCl, 4.7 mM KCl, 1.9 mM $CaCl_2$, 10 mM HEPES at pH 6.9; Ephrussi and Beadle 1936) and fixed in 4% paraformaldehyde (Ted Pella Inc., EM Grade) in PBS with 0.1% DMSO for 1 hr, followed by three rinses in PBS. All washes were carried out for 5 min at room temperature, unless specified otherwise. The tissue was dehydrated by sequential washes into 100% EtOH, frozen indefinitely at −20°C, and rehydrated by sequential washes into PBS. The ovaries were treated with proteinase K (GIBCO BRL) for 1 hr (50 μg/ml of proteinase K in 50 mM Tris/HCl at pH 7.5, 50 mM EDTA), and were washed twice in PBS, 0.2% glycine, once in PBS, and twice in PBT (PBS, 0.1% Tween 20). Samples were postfixed in 5% paraformaldehyde in PBT for 20–30 min and washed five times in PBT, once in 50% PBT/50% hybridization solution, and once in 100% hybridization solution (hybridization solution: 50% formamide, 5× SSC, 50 μg/ml of heparin, 0.1% Tween 20, 100 μg/ml of tRNA, 100 μg/ml of single-stranded DNA). The tissue was prehybridized for 1 hr or more at 48°C in hybridization solution, then hybridized with denatured probe (3 μl = 10–20 ng) in 50 μl hybridization solution overnight at 48°C–50°C. Probe solution was removed, and the tissue was washed once for 20 min at 48°C in hybridization solution, once for 20 min at 48°C in 50% PBT/50% hybridization solution, and five times for 5 min at 48°C in PBT. Anti-digoxigenin–alkaline phosphatase antibody (Boehringer Mannheim) was diluted 1:2000 in PBT (no preabsorption), and incubated with tissue overnight at 4°C. The tissue was washed three times for 5 min in PBT, three times for 20 min in PBT, and twice in buffer 3 (100 mM NaCl, 50 mM $MgCl_2$, 100 mM Tris/HCl at pH 9.5). Color reactions were developed in buffer 3, using 4.5 μl of NBT and 3.5 μl of X-phosphate per milliliter of buffer. Samples were transferred directly from the color reaction solutions into 65% glycerol in PBS and dissected for microscopy.

Digoxigenin-labeled DNA probes were synthesized according to the manufacturer's specifications (Boehringer Mannheim), except that hexamer primers (pd$[N]_6$, Pharmacia) were added to a final concentration of 9 OD/ml to generate probes of shorter length. Labeling was carried out with 50–100 ng of gel-purified template DNA, and 1/10 (10–20 ng) of the generated probe was used per sample.

Microtubule visualization

A protocol for microtubule fixation and staining was modified from Theurkauf et al. (1992) and Lane and Kalderon (1994). Females (2–5 days old) were dissected at room temperature in modified Robb's medium (Theurkauf et al. 1992) and fixed in −20°C methanol for 10 min. The tissue was rinsed three times in 1× PBS and extracted for 2 hr with 1% saponin in PBS. The ovaries were rinsed twice in 0.05% saponin in PBS (PBSS) and incubated for 48 hr at 4°C in a 1:500 dilution of monoclonal anti-α-Tubulin antibody (Sigma, clone DM 1A) in PBSS. The samples were rinsed four times for 15 min each in PBSS at room temperature and incubated with a 1:100 dilution of BODIPY-conjugated goat anti-mouse secondary antibody (Molecular Probes) in PBSS overnight at 4°C or for 2 hr at room temperature. The samples were subsequently rinsed four times for 15 min each in PBSS, and dehydrated and mounted as described in Theurkauf et al. (1992).

Staining was observed on a Bio-Rad MRC-600 confocal microscope, utilizing the Bio-Rad COMOS program. Images were processed with NIH Image.

Molecular analysis

DNA flanking the P element was isolated from a λ library as follows: Total genomic DNA from hls^{3987} adults was cut to completion with *Eco*RI, ligated into λ arms (Stratagene), and packaged using the Gigapack Gold commercial extract from Stratagene. The library was screened with sequences from the 5′ end of the transposon, and 13 positive plaques were obtained. From one such phage, a 2.1-kb *Eco*RI fragment that contained 0.55 kb of 5′ P-element sequences, and 1.55 kb of genomic DNA flanking the P element was subcloned into Bluescript KS(+) (Stratagene). The flanking DNA was digested with *Rsa*I and *Cla*I to obtain a fragment specific for the genomic DNA. This 0.9-kb *Rsa*I–*Cla*I fragment was then used to probe two cosmid libraries (generous gifts of Max Scott (Massey University, Palmerston North, New Zealand) and Mark Champe). The cosPneo Mark Champe library yielded two positive cosmids, MC1 and MC3.

Northern analysis using a 6.5-kb *Bgl*II cosmid fragment encompassing the P-element insertion site revealed a putative *hls* transcript of 4.6 kb. A nearly full-length cDNA was isolated from an ovarian λgt22A library (Stroumbakis et al. 1994; generous gift of Peter Tolias, Public Health Research Institute, NY), using this same *Bgl*II fragment as a probe. Using sites within the polylinker (*Sal*I, 5′ end; *Not*I, 3′ end), the 4.6-kb cDNA was subcloned into Bluescript KS(+), resulting in the construct pcD5.

Exonuclease III was used to construct a 5′ and a 3′ deletion series from pcD5 in a modification of the protocol described by Sambrook et al. (1989). Time-point samples were removed from exonuclease III treatment and added to tubes containing mung bean nuclease 1 buffer (30 mM Na-acetate at pH 4.6, 50 mM NaCl, 1 mM $Zn(acetate)_2$, 0.001% Triton X-100), and heat killed

at 70°C for 15 min. Mung bean nuclease I (130 units; Boehringer Mannheim) then was added to each sample and incubated at 30°C for 30 min, followed by addition of a stop mixture (0.3 M Tris, 50 mM EDTA at pH 8.0). The ends of the DNA were repaired by Klenow treatment as described by Sambrook et al. (1989), and samples were phenol-extracted in the presence of 40 mM Tris at pH 9.5, 640 mM LiCl, and 0.32% SDS. Samples then were precipitated and resuspended in ligation buffer.

Sequencing was carried out by the dideoxy chain termination method using Sequenase, version 2.0 (U.S. Biochemical), following the manufacturer's specifications. Sequence was compiled using the IntelliGenetics program. Data base searches with protein sequences were carried out using the BLAST program from the National Institutes of Health (NIH) (Altschul et al. 1990), and alignments were generated with the GCG program (University of Wisconsin, Madison).

Nucleic acid hybridization

Total RNA was prepared by the hot phenol method (Jowett 1986). RNA (35 μg) was loaded in each lane and transferred to Zeta-Probe membrane (Bio-Rad). Hybridization at 42°C was according to Sambrook et al. (1989), with the addition of 0.225 mg/ml of single-stranded DNA and 0.1 mg/ml of tRNA in the hybridization buffer.

Acknowledgments

We are grateful to Drs. Paul Schedl, Trudi Schüpbach, Bob Cohen, Lynn Cooley, and Ruth Steward for providing cDNAs, Daniel St. Johnston, Hannele Ruohola-Baker, and Jim Kennison for providing stocks, and Peter Tolias, Mark Champe, and Max Scott for providing libraries. We acknowledge the work of Todd Enderlin for help in sequencing regions of *hls* genomic DNA and Jennifer Sledge for aid in analyzing the hls^{E616} and hls^{E653} mutants. Special thanks go to Drs. Susan Parkhurst and Bob Braun and members of the Berg laboratory for critical review of the manuscript and to Drs. Heidi Horowitz and Deanna Frost for technical advice. This work was supported by NIH grants RO1 GM45248 and T32 GM07735.

The publication costs of this article were defrayed in part by payment of page charges. This article must therefore be hereby marked "advertisement" in accordance with 18 USC section 1734 solely to indicate this fact.

References

Altschul, S.F., W. Gish, W. Miller, E. Myers, and D. Lipman. 1990. Basic local alignment search tool. *J. Mol. Biol.* **215**: 403–410.

Anderson, K. 1995. One signal, two body axes. *Science* **269**: 489–490.

Berleth, T., M. Burri, G. Thoma, D. Bopp, S. Richstein, G. Frigerio, M. Noll, and C. Nüsslein-Volhard. 1988. The role of localization of *bicoid* RNA in organizing the anterior pattern of the *Drosophila* embryo. *EMBO J.* **7**: 1749–1756.

Belote, J.M. and J.C. Lucchesi. 1980. Male-specific lethal mutations of *Drosophila melanogaster*. *Genetics* **96**: 165–186.

Burgess, S., J.R. Couto, and C. Guthrie. 1990. A putative ATP binding protein influences the fidelity of branchpoint recognition in yeast splicing. *Cell* **60**: 705–717.

Chasan, R. and K.V. Anderson. 1993. Maternal control of dorsal/ventral polarity and pattern in the embryo. In *The development of* Drosophila melanogaster. (ed. M. Bate and A. Martinez-Arias), pp. 387–424. Cold Spring Harbor Laboratory Press, Cold Spring Harbor, New York.

Chen, J.-H. and R.-J. Lin. 1990. The yeast PRP2 protein, a putative RNA-dependent ATPase, shares extensive sequence homology with two other pre-mRNA splicing factors. *Nucleic Acids Res.* **18**: 6447.

Cheung, H.-K., T.L. Serano, and R.S. Cohen. 1992. Evidence for a highly selective RNA transport system and its role in establishing the dorsoventral axis of the *Drosophila* egg. *Development* **114**: 653–661.

Christerson, L.B. and D.M. McKearin. 1994. *orb* is required for anteroposterior and dorsoventral patterning during *Drosophila* oogenesis. *Genes & Dev.* **8**: 614–628.

Clark, I., E. Giniger, H. Ruohola-Baker, L.Y. Jan, and Y.N. Jan. 1994. Transient posterior localization of a kinesin fusion protein reflects anteroposterior polarity of the *Drosophila* oocyte. *Curr. Biol.* **4**: 289–300.

Ding, D., S.M. Parkhurst, S.R. Halsell, and H.D. Lipshitz. 1993a. Dynamic *Hsp83* RNA localization during *Drosophila* oogenesis and embryogenesis. *Mol. Cell. Biol.* **13**: 3773–3781.

Ding, D., S.M. Parkhurst, and H.D Lipshitz. 1993b. Different genetic requirements for anterior RNA localization revealed by the distribution of ADDUCIN-like transcripts during *Drosophila* oogenesis. *Proc. Natl. Acad. Sci.* **90**: 2512–2516.

Ephrussi, A., L.K. Dickinson, and R. Lehmann. 1991. *oskar* organizes the germ plasm and directs localization of the posterior determinant *nanos*. *Cell* **66**: 37–50.

Ephrussi, B. and G.W. Beadle. 1936. A technique of transplantation for *Drosophila*. *Am. Nat.* **70**: 218–225.

González-Reyes, A. and D. St. Johnston. 1994. Role of oocyte position in establishment of anterior-posterior polarity in *Drosophila*. *Science* **266**: 639–642.

González-Reyes, A., H. Elliott, and D. St. Johnston. 1995. Polarization of both major body axes in *Drosophila* by *gurken-torpedo* signalling. *Nature* **375**: 654–658.

Gutzeit, H. and R. Koppa. 1982. Time-lapse film analysis of cytoplasmic streaming during late oogenesis of *Drosophila*. *J. Embryol. Exp. Morphol.* **67**: 101–111.

Hodgman, T.C. 1988. A new superfamily of replicative proteins [letter]. [published erratum appears in *Nature* 1988. **333**: 578] *Nature* **333**: 22–23.

Jowett, T. 1986. Preparation of nucleic acids. In Drosophila: *A practical approach* (ed. D.B. Roberts), pp. 275–286. IRL Press, Oxford, UK.

Karpen, G.H. and A.C. Spradling. 1992. Analysis of subtelomeric heterochromatin in the *Drosophila* minichromosome Dp1187 by single *P* element insertional mutagenesis. *Genetics* **132**: 737–753.

Kim, S.H. and R.-J. Lin. 1993. Pre-mRNA splicing within an assembled yeast spliceosome requires an RNA-dependent ATPase and ATP hydrolysis. *Proc. Natl. Acad. Sci.* **90**: 888–892.

Kim, S.-H., J. Smith, A. Claude, and R.-J. Lin. 1992. The purified yeast pre-mRNA splicing factor PRP2 is an RNA-dependent NTPase. *EMBO J.* **11**: 2319–2326.

Kim-Ha, J., J.L. Smith, and P.M. Macdonald. 1991. *oskar* mRNA is localized to the posterior pole of the *Drosophila* oocyte. *Cell* **66**: 23–35.

Kloc, M. and L.D. Etkin. 1995. Delocalization of Vg1 mRNA from the vegetal cortex in *Xenopus* oocytes after destruction of Xlsirt RNA. *Science* **265**: 1101–1103.

Koch, E.A. and R.H. Spitzer. 1983. Multiple effects of colchicine on oogenesis in *Drosophila*: Induced sterility and switch of potential oocyte to nurse-cell developmental pathway. *Cell Tissue Res.* **228**: 21–32.

Kuroda, M.I., M.J. Kernan, R. Kreber, B. Ganetzky, and B.S. Baker. 1991. The *maleless* protein associates with the X chromosome to regulate dosage compensation in *Drosophila*. *Cell* **66**: 935–947.

Lane, M.E. and D. Kalderon. 1994. RNA localization along the

anteroposterior axis of the *Drosophila* oocyte requires PKA-mediated signal transduction to direct normal microtubule organization. *Genes & Dev.* **8**: 2986–2995.

Lantz, V., L. Ambrosio, and P. Schedl. 1992. The *Drosophila orb* gene is predicted to encode sex-specific germline RNA-binding proteins and has localized transcripts in ovaries and early embryos. *Development* **115**: 75–88.

Lasko, P. and M. Ashburner. 1988. The product of the *Drosophila* gene *vasa* is very similar to eukaryotic initiation factor-4A. *Nature* **335**: 611–617.

Lee, C.-G. and J. Hurwitz. 1993. Human RNA helicase A is homologous to the maleless protein of *Drosophila*. *J. Biol. Chem.* **268**: 16822–16830.

Lehmann, R. and C. Nüsslein-Volhard. 1991. The maternal gene *nanos* has a central role in posterior pattern formation of the *Drosophila* embryo. *Development* **112**: 679–691.

Lin., H., L. Yue, and A. Spradling. 1994. The *Drosophila* fusome, a germline-specific organelle, contains membrane skeletal proteins and functions in cyst formation. *Development* **120**: 947–956.

Lindsley, D.L. and G.G. Zimm. 1992. *The genome of* Drosophila melanogaster. Academic Press, San Diego, CA.

Litman, P., J. Barg, and I. Ginzburg. 1994. Microtubules are involved in the localization of *tau* mRNA in primary neuronal cell cultures. *Neuron* **13**: 1463–1474.

Lohs-Schardin, M. 1982. *Dicephalic*, a *Drosophila* mutant affecting polarity in follicle organization and embryonic patterning. *Wilhelm Roux's Arch. Dev. Biol.* **191**: 28–36.

Mahowald, A.P. 1962. Fine structure of pole cells and polar granules in *Drosophila melanogaster*. *J. Exp. Zool.* **151**: 201–205.

Neuman-Silberberg, F.S. and T. Schüpbach. 1993. The *Drosophila* dorsoventral patterning gene *gurken* produces a dorsally localized RNA and encodes a TGFα-like protein. *Cell* **75**: 165–174.

Peifer M., S. Orsulic, L.M. Pai, and J. Loureir. 1993. A model system for cell adhesion and signal transduction in *Drosophila*. *Development* (Suppl.) **1**: 163–176.

Pokrywka, N.J. and E.C. Stephenson. 1991. Microtubules mediate the localization of bicoid RNA during *Drosophila* oogenesis. *Development* **113**: 55–66.

———. 1995. Microtubules are a general component of mRNA localization systems in *Drosophila* oocytes. *Dev. Biol.* **167**: 363–370.

Ran, B., R. Bopp, and B. Suter. 1994. Null alleles reveal novel requirements for *Bic-D* during *Drosophila* oogenesis and zygotic development. *Development* **120**: 1233–1242.

Robertson, H.M., C.R. Preston, R.W. Phillis, D.M. Johnson-Schlitz, W.K. Benz, and W.R. Engels. 1988. A stable genomic source of *P* element transposase in *Drosophila melanogaster*. *Genetics* **118**: 461–470.

Roth, S., F.S. Neuman-Silberberg, G. Barcelo, and T. Schüpbach. 1995. *cornichon* and the EGF receptor signaling process are necessary for both anterior-posterior and dorsal-ventral pattern formation in *Drosophila*. *Cell* **81**: 967–978.

Ruohola, H., K.A. Bermer, D. Baker, F.R. Swedlow, L.Y. Jan, and Y.N. Jan. 1991. Role of neurogenic genes in establishment of follicle cell fate and oocyte polarity during oogenesis in *Drosophila*. *Cell* **66**: 433–449.

Sambrook, J., E.F. Fritsch, and T. Maniatis. 1989. *Molecular cloning: A laboratory manual*, 2nd ed. Cold Spring Harbor Laboratory Press, Cold Spring Harbor, New York.

Schüpbach, T. and S. Roth. 1994. Dorsoventral patterning in *Drosophila* oogenesis. *Curr. Opin. Genet. Dev.* **4**: 502–507.

Schüpbach, T. and E. Wieschaus. 1991. Female sterile mutations on the second chromosome of *Drosophila melanogaster*. II. Mutations blocking oogenesis or altering egg morphology. *Genetics* **129**: 1119–1136.

Schwer, B. and C. Guthrie. 1991. PRP16 is an RNA-dependent ATPase that interacts transiently with the spliceosome. *Nature* **349**: 494–499.

Shuman, S. 1992. Vaccinia virus RNA helicase: An essential enzyme related to the DE-H family of RNA-dependent NTPases. *Proc. Natl. Acad. Sci.* **89**: 10935–10939.

Spradling, A.C. 1993. Developmental genetics of oogenesis. In *The development of* Drosophila melanogaster (ed. M. Bate and A. Martinez-Arias), pp. 1–70. Cold Spring Harbor Laboratory Press, Cold Spring Harbor, New York.

Stephenson, E.C. and N.J. Pokrywka. 1992. Localization of *bicoid* message during *Drosophila* oogenesis. *Curr. Top. Dev. Biol.* **26**: 23–34.

Steward, R. and C. Nüsslein-Volhard. 1986. The genetics of the *dorsal-Bicaudal-D* region of *Drosophila melanogaster*. *Genetics* **113**: 665–678.

St. Johnston, D. 1993. Pole plasm and the posterior group genes. In *The development of* Drosophila melanogaster (ed. M. Bate and A. Martinez-Arias), pp. 325–363. Cold Spring Harbor Laboratory Press, Cold Spring Harbor, New York.

St. Johnston, D., W. Driever, T. Berleth, S. Richstein, and C. Nüsslein-Volhard. 1989. Multiple steps in the localization of *bicoid* RNA to the anterior pole of the *Drosophila* oocyte. *Development* (Suppl.) **1**: 13–19.

St. Johnston, D., D. Beuchle, and C. Nüsslein-Volhard. 1991. *staufen*, a gene required to localize maternal RNAs in the *Drosophila* egg. *Cell* **66**: 51–63.

Stroumbakis, N.D., Z. Li, and P.P. Tolias. 1994. RNA- and single-stranded DNA-binding (SSB) proteins expressed during *Drosophila melanogaster* oogenesis: A homolog of bacterial and eukaryotic mitochondrial SSBs. *Gene* **143**: 171–177.

Suter, B., L.M. Romber, and R. Steward. 1989. *Bicaudal-D*, a *Drosophila* gene involved in developmental asymmetry: Localized transcript accumulation in ovaries and sequence similarity to myosin heavy chain rail domains. *Genes & Dev.* **3**: 1957–1968.

Tearle, R. and C. Nüsslein-Volhard. 1987. Tübingen mutants and stocklist. *Dros. Inf. Serv.* **66**: 209–269.

Theurkauf, W.E. 1994a. Microtubules and cytoplasm organization during *Drosophila* oogenesis. *Dev. Biol.* **165**: 352–360.

———. 1994b. Premature microtubule-dependent cytoplasmic streaming in *cappuccino* and *spire* mutant oocytes. *Science* **265**: 2093–2096.

Theurkauf, W.E., S. Smiley, M.L. Wong, and B.M. Alberts. 1992. Reorganization of the cytoskeleton during *Drosophila* oogenesis: Implications for axis specification and intercellular transport. *Development* **115**: 923–936.

Theurkauf, W.E., B. Alberts, Y.N. Jan, and T. Jongens. 1993. A central role for microtubules in the differentiation of *Drosophila* oocytes. *Development* **118**: 1169–1180.

Wang, C. and R. Lehmann. 1991. *nanos* is the localized posterior determinant in *Drosophila*. *Cell* **66**: 637–647.

Wieschaus, E., J.L. Marsh, and W. Gehring. 1978. *fs(1)K10*, a germline-dependent female sterile mutation causing abnormal chorion morphology in *Drosophila melanogaster*. *Wilhelm Roux's Arch. Dev. Biol.* **184**: 75–82.

Yisraeli, J.K., S. Sokol, and D.A. Melton. 1990. A two-step model for the localization of maternal mRNA in *Xenopus* oocytes: Involvement of microtubules and microfilaments in the translocation and anchoring of Vg1 mRNA. *Development* **108**: 289–298.

Yue, L. and A. Spradling. 1992. *hu-li tai shao*, a gene required for ring canal formation during *Drosophila* oogenesis, encodes a homolog of adducin. *Genes & Dev.* **6**: 2443–2454.

Homeless is required for RNA localization in Drosophila oogenesis and encodes a new member of the DE-H family of RNA-dependent ATPases.

D E Gillespie and C A Berg

Genes Dev. 1995 9: 2495-2508
Access the most recent version at doi:10.1101/gad.9.20.2495